Davaadorj et al., Cell Dev Biol 2017, 6:3
DOI: 10.4172/2168-9296.1000188

Cell & Developmental Biology

Research Article Open Access

Impaired Autophagy in Retinal Pigment Epithelial Cells Induced from iPS Cells obtained from a Patient with Sialidosis

Odontuya Davaadorj[1,3], Hisako Akatsuka[1,2], Yoshiki Yamaguchi[1], Chisa Okada[4], Masatoshi Ito[4], Nahoko Fukunishi[4], Yoshiki Sekijima[5], Hideki Ohnota[6], Kenji Kawai[3], Takahiro Suzuki[3], Takehito Sato[1]* and Yasuyuki Suzuki[3]

[1]*Department of Host Defense Mechanism, Tokai University School of Medicine, Kanagawa, Japan*
[2]*Department of Molecular Life Science, Division of Basic Medical Science and Molecular Medicine, Tokai University School of Medicine, Kanagawa, Japan*
[3]*Department of Ophthalmology, Tokai University School of Medicine, Kanagawa, Japan*
[4]*Support Center for Medical Research and Education, Tokai University, Kanagawa, Japan*
[5]*Department of Medicine (Neurology and Rheumatology), Shinshu University School of Medicine, Nagano, Japan*
[6]*Department of Drug Discovery Science, Shinshu University School of Medicine, Nagano, Japan*

Abstract

Sialidosis type I patient-derived induced pluripotent stem cells (iPSCs) were generated from blood mononuclear cells. During embryoid body-like 3D culture, aggregates of patient-derived iPSCs were irregular in shape and had increased vacuoles filled with lipid droplets and cellular components such as damaged mitochondria. Retinal pigment epithelial cells induced from patient-derived iPSCs showed impaired autophagy flux with decreased formation of LC3 puncta. Sialidosis patient-derived iPSCs could provide a useful tool for investigating the mechanism of the autophagy/lysosome-mediated degradation system.

Keywords: Retinal pigment epithelium; Sialidosis; Autophagy; Cherry red spot; LC3; iPSC

Introduction

Sialidosis is a lysosomal storage disease caused by mutations of the *N-acetyl-α-neuraminidase-1* (*NEU1*) gene that result in decreased enzymatic activity. NEU1 is a lysosomal sialidase (EC 3.2.1.18) that cleaves the terminal sialic acid in oligosaccharide chains. Decreased NEU1 activity results in the accumulation of sialoglycoconjugates in cells and tissues, leading to various symptoms such as visual impairment, myoclonus, ataxia, seizure, mental retardation and hepatosplenomegaly [1-4]. Sialidosis is classified into two clinical variants with different onset and severity: Type I is a relatively mild form with infantile onset, while type II is an early-onset form with more severe manifestations. Sialidosis is also known as the "cherry-red spot myoclonus syndrome". The cherry-red spot is often observed in lysosomal disorders, manifesting as a whitish circular shape in the perifoveal region. Therefore, ophthalmic fundus examination has been used for clinical diagnosis of sialidosis. The cherry-red spot has been explained as a thickening of the retina [5]; however, pathological mechanisms are not fully understood.

Retinal pigment epithelium (RPE), situated between the neurosensory retina and Bruch's membrane, is critical for retinal homeostasis through nutrient supply, active phagocytosis, and autophagy [6,7]. Shed photoreceptor outer segments (POS) are engulfed by the RPE and the so formed membrane-bound phagosomes subsequently fuse with lysosomes in which the POS are degraded. The resultant molecules are reused for the maintenance of the visual cycle. Kim et al. reported that the degradation of POS in the RPE is closely associated with LC3-mediated autophagy [8]. Autophagy plays an important role in the digestion of damaged cellular components, especially in post-mitotic cells such as the RPE. Therefore, autophagy is pivotal, not only for intra-cellular homeostasis, but also for retinal integration. Since lysosomes are the site at which the final stage of autophagy takes place, deficiency of the lysosomal enzyme NEU1 may affect this process. It is plausible that a symptom of sialidosis, the cherry-red spot, may be related to the dysfunction of the RPE. In this study, we generated sialidosis patient-derived iPSCs, from which RPE cells were induced in order to examine the effect of NEU1 deficiency on the process of autophagy.

Materials and Methods

Generation of type I sialidosis patient-derived iPSCs

Mononuclear cells obtained from the peripheral blood of a sialidosis type I patient [4] were stimulated by anti-CD3/CD28 coated beads (DB11131, Thermo Fisher Scientific, Waltham, MA, USA) in the presence of rIL-2 (Novartis, Basel, Switzerland). The cells were transduced with reprogramming factors via the Sendai virus vector SeVdp(KOSM) [9,10] and cultured on mitomycin C-treated mouse embryonic fibroblasts in DMEM F12 (D6421, Sigma-Aldrich, St. Louis, MO, USA) containing 20% KnockOut Serum Replacement (KSR; 10828-028, GIBCO, Thermo Fisher Scientific), 1% nonessential amino acids (11140, GIBCO, Thermo Fisher Scientific), 1x L-glutamine-penicillin-streptomycin (G1146, Sigma-Aldrich) and 5 ng/mL bFGF (060-04543, Wako Chemicals, Neuss, Germany). The generated iPSC colonies were harvested and expanded. This study was approved by the ethics board of Tokai University Hospital in Japan.

In vitro differentiation of iPSCs

For proving the mesodermal differentiation potential, iPSCs were transferred to feeder-free conditions and cultured in RPMI1640/B27 medium containing 10 ng/mL bFGF, 5 ng/mL activin A, 10 ng/mL BMP4 and 5 μM CHIR99021 for 2 days. For endodermal differentiation, iPSCs were cultured with 100 ng/mL activin A and 5 μM CHIR99021 for 1 day and with 100 ng/mL activin A for another 3 days. Differentiation to RPE cells was induced as previously described by Takahashi's group [11] with slight modification. Briefly, dissociated clumps of iPSC colonies were cultured in non-adherent dishes (Prime Surface dish #MS-9035X,

***Corresponding author:** Takehito Sato, Department of Host Defense Mechanism, Tokai University School of Medicine, Kanagawa, Japan, Tel: +81-463-93-1121; Ext. 2593; Fax: +81-463-94-2976; E-mail: takehito@is.icc.u-tokai.ac.jp

Received August 23, 2017; **Accepted** August 29, 2017; **Published** September 05, 2017

Citation: Davaadorj O, Akatsuka H, Yamaguchi Y, Okada C, Ito M, et al. (2017) Impaired Autophagy in Retinal Pigment Epithelial Cells Induced from iPS Cells obtained from a Patient with Sialidosis. Cell Dev Biol 6: 188. doi:10.4172/2168-9296.1000188

Sumitomo Bakelite, Tokyo, Japan) with DMEM F12 containing 20% KSR, 0.1 mM 2-ME, 1x non-essential amino acids (11140-050, GIBCO) and 2 mM L-Glutamate for 3 days, then cultured in ES differentiation medium (GMEM, 0.1 mM non-essential amino acids, 1 mM pyruvate, and 0.1 mM 2-Mercaptoethanol) containing 20% KSR for 3 days, then in GMEM containing 15% KSR for 9 days and in GMEM containing 10% KSR for 6 days. Finally, CKI-7 (final 5 μM) and SB431542 (final 5 μM) were added to the medium and the medium was changed every 2 days. RPE cells emerged approximately after three weeks of culturing.

Immunocytochemistry

Cells were fixed with 4% paraformaldehyde for 30 min at room temperature and washed with PBS. The fixed cells were incubated in PBS containing 5% goat serum with 0.5% Triton X-100. Then, the cells were incubated with the primary antibody or biotinylated lectin in PBS containing 1% goat serum and 0.5% Triton X-100 overnight at 4°C. After washing with PBS 3 times, the cells were incubated with Alexa Fluor 488-labeled secondary antibodies for 2 h at room temperature. Thereafter, the cells were washed with PBS 3 times and counter-stained with DAPI for 15 min. Photomicrographs were taken using a microscope (Carl Zeiss Axio Vert A1). The following primary antibodies and lectin were used: anti-LC3 pAb (PM036, MBL International, Woburn, MA, USA), anti-SSEA-4 (#MAB4304, Millipore, Billerica, MA, USA), anti-TRA-1-60 (#MAB4360, Millipore), anti-TRA-1-81 (#MAB4381, Millipore), rabbit anti-ZO1 (#33-9100, Thermo Fisher Scientific), anti-hSOX17 (#MAB1924, R&D system, MN, USA), anti-MESP1 (#ab129387, Abcam, Tokyo Japan) and biotin-labelled wheat germ agglutinin (WGA; #B-1025, Vector Labs, Burlingame, CA, USA). Alexa Fluor 488-/Alexa Fluor 594-labeled anti-mouse IgG (A-11017 and A-11020, respectively, Thermo Fisher Scientific) and anti-rabbit IgG (A-11070 and A-11072, respectively, Thermo Fisher Scientific) were used as secondary antibodies. Cell nuclei were counterstained with DAPI (1 μg/mL). The numbers and areas of LC3 puncta were measured and calculated by the Cellomics ArrayScan VTI cell image analyzer (Thermo Fisher Scientific) and Cellomics Scan/View program (Thermo Fisher Scientific). Alkaline phosphatase was detected using alkaline phosphatase substrate kit II (#SK-5200, Vector Labs).

Transmission Electron Microscopy (TEM)

The cells were fixed in 2.5% 0.05 M phosphate buffer for 2 h and post fixed in 1% osmium tetroxide/0.05 M phoaphate buffer for 1 h, then stained with uranyl acetate. After dehydration with a graded ethanol series, specimens were embedded in Quetol 812. Semi-thin sections were stained with toluidine blue, and suitable areas for ultrastructural study were chosen under a light microscope. Ultrathin sections were stained with uranyl acetate and lead citrate and examined using a transmission electron microscope (JEM 1400, JEOL, Tokyo, Japan).

qPCR

Total RNA was extracted using the TRIzol reagent (Invitrogen, Carlsbad, CA, USA). cDNA was synthesized using Super Script III Master Mix VILO reverse transcriptases (11754-050 and 11754-250, Invitrogen) with random hexamer primers. Quantitative real-time PCR was performed using the TOYOBO PCR Master Mix (QPS-201, THUNDERBIRD, SYBR, Toyobo Global, Osaka, Japan) on an ABI Fast 7500 machine (Applied Biosystems, Carlsbad, CA, USA). The data were analyzed by the ΔΔCt method. Primer sequences are listed in Table 1.

Western blot analysis

Cells were lysed in RIPA buffer (50 mM Tris-HCl, pH 7.5, 150 mM NaCl, 1% NP-40, 1% Sodium deoxycholate, 0.1% SDS and protease inhibitor cocktail). Proteins were separated by SDS-PAGE on 12.5% gels and wet-blotted onto PVDF membranes (IPVH304FO, Immobilon, Millipore). After blocking in TBS-T containing 5% skim milk, membranes were incubated with antibodies against LC3 (PM036, MBL International) and β-actin (#A5441, Sigma-Aldrich). The membranes were washed with TBS-T 3 times and then incubated with HRP-labeled anti-rabbit IgG and anti-mouse IgG. Enhanced chemiluminescence signals were visualized and quantified using ImageJ software.

Gene	Primer sequences (5'-3')	
	Forward	Reverse
CRALBP	AGATCTCAGGAAGATGGTGGAC	GAAGTGGATGGCTTTGAACC
MITF	AGAGTCTGAAGCAAGAGCACTG	TGCGGTCATTTATGTTAAATCTTC
4-Oct	GCAAAACCCGGAGGAGGAGTC	CCACATCGGCCTGTGTATATC
PAX6	TCACCATGGCAAATAACCTG	CAGCATGCAGGAGTATGAGG
RPE65	CAATGGGTTTCTGATTGTGGA	CCAGTTCTCACGTAAATTGGCTA
RX	GGCAAGGTCAACCTACCAGA	CTTCATGGAGGACACTTCCAG
β-actin	ATTGGCAATGAGCGGTTC	GGATGCCACAGGACTCCA

Table 1: Primer sequences used for qPCR analysis.

Statistical analysis

Data were analyzed using GraphPad Prism software (GraphPad Software, La Jolla, CA, USA). Student's t-test was used for analyzing western blot, real-time quantitative RT-PCR, and immunofluorescence data. Results are presented as mean ± SD. *P*-values ≤ 0.05 were considered statistically significant.

Results and Discussion

Generation of sialidosis type I patient-derived iPSCs

Blood mononuclear cells were obtained from a Japanese 18-year old patient with sialidosis type I harboring a heterozygous missense mutation of c.239C>T and c.403G>A in the *NEU1* gene [4]. After stimulation with anti-CD3 and anti-CD28 coated micro beads along with IL-2, reprogramming factors Oct3/4, Sox2, Klf4 and c-myc were introduced via a sendaivirus vector [9,10]. Then, the cells were cultured on mouse embryonic fibroblasts (MEF) in the presence of bFGF and KSR. Colonies that displayed typical iPSC-like morphology were harvested and expanded. Immunofluorescence analysis revealed that the cells expressed pluripotent cell markers SSEA-4, TRA-1-60 and TRA1-81. Another stem cell marker, alkaline phosphatase, was also detected (Figure 1A). These mononuclear cell-derived cells grew well on MEF with bFGF and 20% KSR and could differentiate into Pax6-expressing ectodermal lineage cells, Sox17-expressing endodermal lineage cells (Figure1B) and MESP-1-expressing mesoderm lineage cells (Figure 1C), suggesting that the cells had self-renewal activity and multipotency.

Deformed embryoid bodies of patient-derived cells

In order to induce the differentiation to RPE cells, healthy donor-derived (control) and patient-derived iPSCs were collected, and small cell clumps were cultured in non-adhesive dishes with differentiation media. After 21 days of culture, while aggregates of control cells showed well-packed, round embryoid body (EB)-like structures (Figures 2A(a) and 2A(d)), the patient-derived cell aggregates had less tightly packed EB-like structures of irregular shape (Figures 2A(b), 2A(c), 2A(e) and 2A(f)). Aggregates of patient-derived cells were easily dissociated by gentle pipetting, indicating impaired cell adhesion. This is consistent with the evidence that the increased amount of sialic acid on proteins and glycolipids is associated with tumor malignancy and metastasis, partly due to decreased cell adhesion [12,13].

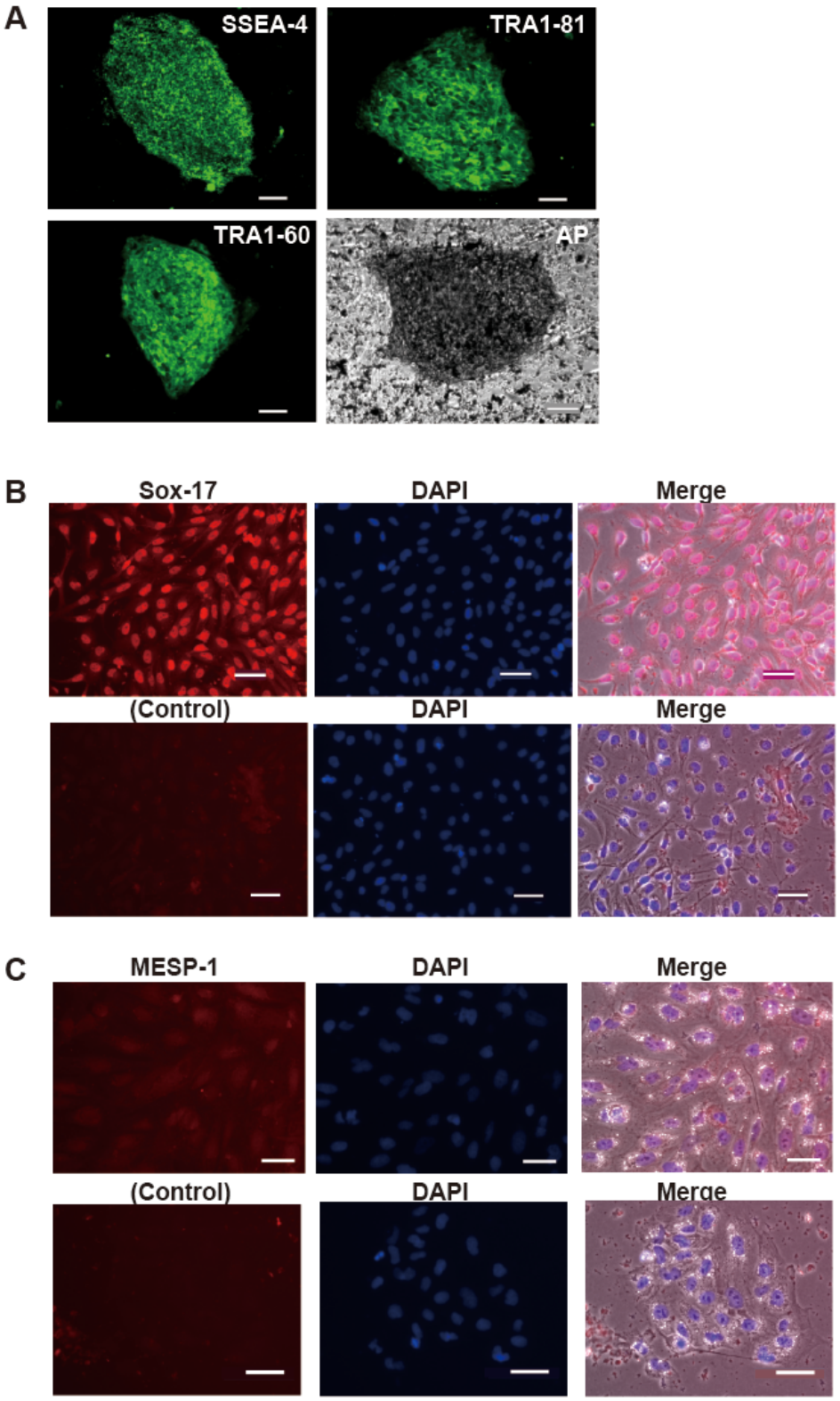

Figure 1: Characterization of induced pluripotent stem cells (iPSCs) derived from a sialidosis type I patient. (A) Patient-derived iPS cell line expressed pluripotency markers, SSEA-4, TRA1-81 and TRA1-60 and showed alkaline phosphatase activity (AP). Scale bars, 200 μm. Patient-derived iPS cells could be induced to Sox-17-expressing endodermal progenitors (B) and to MESP1-expressing mesodermal progenitors (C). As negative controls, Rabbit IgG was used in place of 1st antibodies (Control). Alexa Fluor 594 (Sox-17 or MESP-1), DAPI, and merged data with bright field (Merge) are shown. Scale bars, 50 μm (B, C).

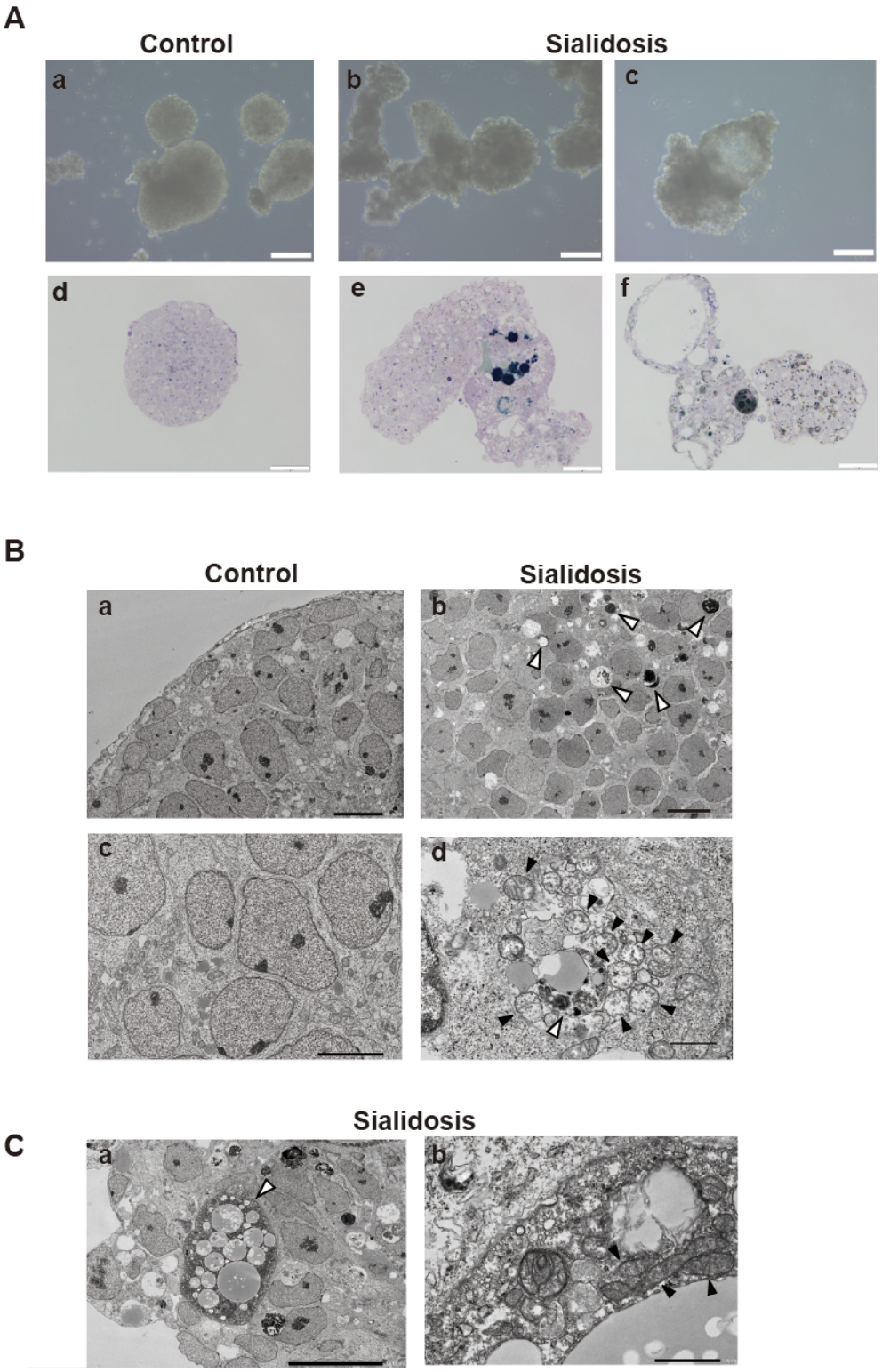

Figure 2: Aberrant morphology of patient-derived embryoid bodies (EB).
(A) Small clumps of iPSCs were cultured in non-adhesive dish in differentiation medium for 21 days. While control iPS cells formed tightly packed EB-like structure (a), sialidosis patient-derived cells formed irregular shaped EBs (b, c). Toluidine blue-stained sections (d-f) showed some strongly-stained portions in patient derived EBs. Scale bars, 50 μm. (B) In transmission electron microscopy, vacuoles containing electron-dense materials or lamellar structures were frequently found in patient-derived cells (b, white arrowheads). Lysosome filled with lipid droplets and dense materials (d, white arrowhead) were surrounded by damaged mitochondria (d, black arrowheads) in patient-derived cells. Scale bars, 10 μm (a, b), 5 μm (c), and 2 μm (d). (C) Structures strongly stained with toluidine blue (a, white arrowhead) included lipid droplets and mitochondria (b, black arrowheads). Scale bars, 20 μm (a), 1 μm (b).

As shown in Figures 2A(e) and 2A(f), patient-derived aggregates appeared spongy, containing vacuoles of various sizes. In addition, "balloon-like" structures frequently protruded (Figures 2A(c) and 2A(f)). Transmission electron microscopy revealed that vacuoles containing electron-dense materials or lamellar structures were frequent in patient aggregates (Figure 2B(b)). Such vacuoles were often surrounded by lipid droplets and, interestingly, mitochondria with low density, almost lacking cristae (Figure 2B(d)), whereas mitochondria in the control aggregates were electron-dense and rich in cristae (Figure 2B(c)). Since dysfunctional mitochondria are degraded via the autophagy-lysosome pathway (known as mitophagy), the observed accumulation of less dense mitochondria was possibly a result of impaired lysosomal digestion system due to the *NEU1* gene mutation.

Furthermore, portions strongly stained with toluidine blue were often observed inside the patient-derived aggregates (Figures 2A(e) and 2A(f)). These portions contained lipid droplets, lamellar structures and mitochondria (Figure 2C). This phenomenon might also be primarily explained by the impaired lysosomal degradation. However, contribution of enhanced exocytosis is also plausible, since a *Neu1* KO mice study revealed that Neu1 negatively regulates exocytosis through desialylation of the lysosomal protein LAMP1 [14]. Whether Neu1 deficiency affects cellular homeostasis by controlling exocytosis is to be explored in the future.

Impaired autophagy in patient-derived RPE cells

After 21 days of culture, floating cell aggregates of control and patient-derived iPSCs were collected and transferred to laminin-coated adhesive culture plates [11]. Among various cell types, squamous and polygonal cells with pigment appeared after approximately 60 days of culture. These cells were then excised and planted onto another culture plate. The isolated cells grew well and were maintained by serial passages (Figure 3A). The cells exhibited epithelial sheet-like morphology and

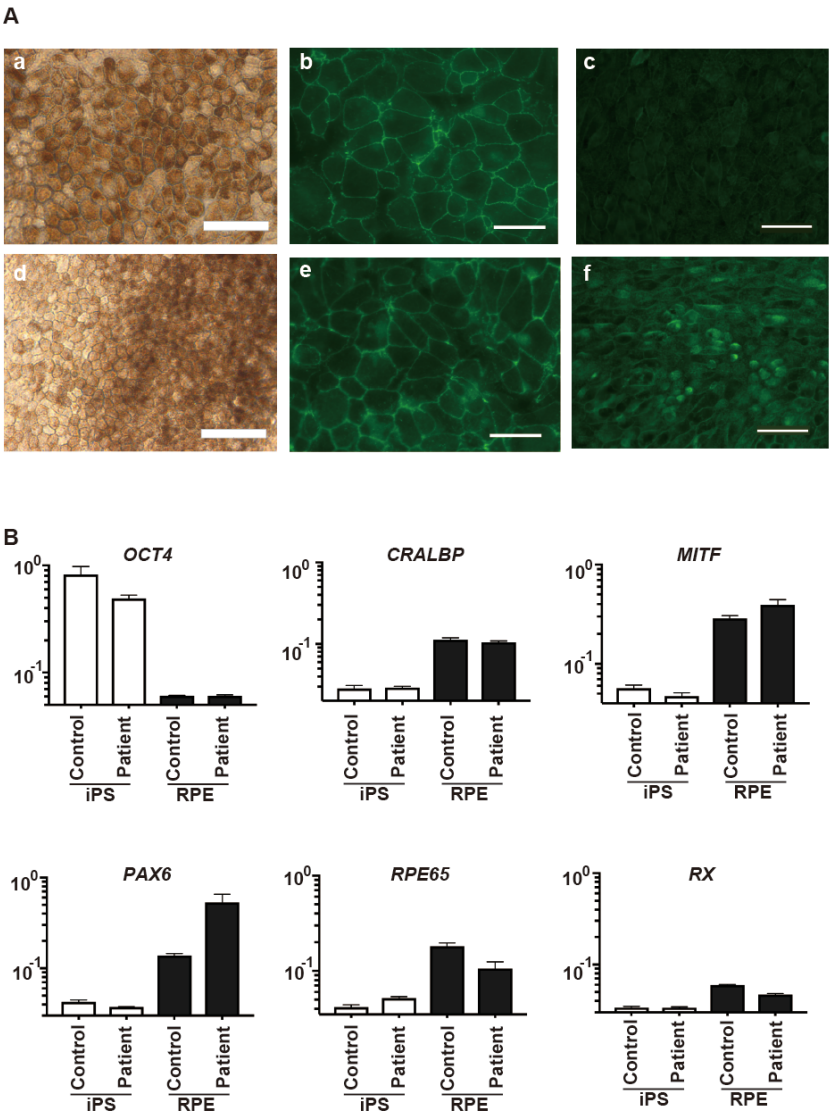

Figure 3: Retinal pigment epithelial (RPE) cells were induced from patient-derived iPSCs.
(A) Phase micrograph showing a tightly packed monolayer of heavily pigmented cells with a polygonal morphology (a, d). Immunocytochemistry analysis using anti-ZO-1 antibody showing that the epithelial tight junctions were formed (b, e). WGA, a ligand for sialic acid, bound strongly to patient-derived cells (c, f). Scale bars, 50 μm. (B) qPCR analysis showing that induced RPE cells expressed ectodermal and RPE markers but not pluripotent markers. White bars are iPSCs. Black bars are RPEs. Data are normalized to β-actin.

had tight junctions, which was confirmed by immunocytochemistry using anti-ZO-1 antibodies reacting with tight junction protein 1 (Figures 3A(b) and 3A(e)). qPCR analysis showed that ZO-1-positive epithelial sheet-like cells from the control and the patient had lost the pluripotent marker Oct3/4, but expressed RPE-specific genes RPE65 and CRALP, as well as neuronal or retinal cell markers Pax6, Rx and MITF, although the expression levels slightly differed between the cell lines (Figure 3) [15,16].

WGA, a ligand for sialic acid, reacted more prominently with sialidosis patient-derived RPE-like cells than with control cells (Figures 3A(c) and 3A(f)), indicating that materials containing sialic acid were accumulated in patient-derived cells, presumably owing to impaired lysosomal activity. Since lysosomal degradation is the final point of the autophagy pathway, impaired lysosomal activity might affect the process of autophagy initiation. A ubiquitin-like protein LC3 is known to be involved in autophagosome formation, the initiation step of autophagy. LC3 is synthesized as proLC3 and then converted into LC3-I by C-terminus processing. Finally, LC3-I is lipidated with

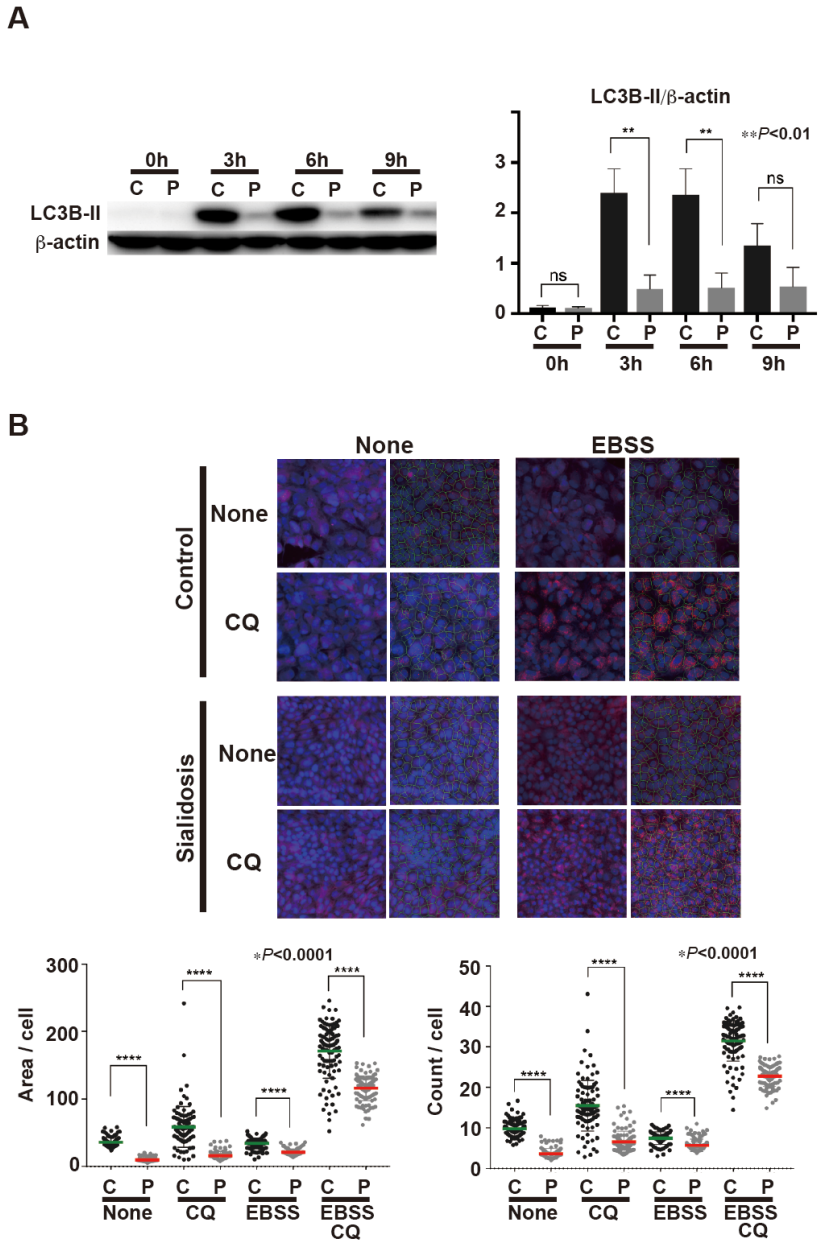

Figure 4: Impaired autophagy in sialidosis patient-derived RPE cells.
(A) Immunoblotting analysis of control (indicated as C) and patient (P) RPEs treated with EBSS and chloroquine for 0, 3, 6, and 9 h. The ratios of band intensities of LC3B-II to β-actin were calculated. Average ± standard deviation of 3 independent experiments is shown. Asterisks indicate a significant difference compared to control cells (**; P<0.01, ns; not significant) (B) RPE cells treated with or without EBSS and chloroquine for 3 h were fixed and stained with anti-LC3 (upper, red). Putative cell border calculated using Cellomics Scan/View program is indicated (upper, green lines). The numbers and areas of LC3 puncta (C; control, P; patient) were measured by a cell image analyzer. The values per cell in each visual field were calculated and plotted as dots (n=200). Averages ± standard errors are indicated as horizontal bars and error bars, respectively. Asterisks indicate a significant difference compared to control cells (****; P<0.0001).

phosphatidylethanolamine or phosphatidylserine to become LC3-II, which associates with the autophagosome/autolysosome membrane. We first examined whether starvation induced LC3-II in patient-derived RPE-like cells. Both cell populations were subjected to starvation in Earle's balanced salt solution (EBSS) in the presence of chloroquine (CQ) for 3, 6 and 9 h (Figures 4A(a) and 4A(b)). LC3-II induction was prominent in control cells, but quite weak in patient-derived cells, suggesting that the patient-derived cells were defective with respect to autophagy induction.

To confirm this, autophagosome formation was examined by measuring punctate LC3 using a cell image analyzer. The number and area of LC3 puncta per cell in each observed field was calculated (Figure 4B, upper), and the values of 200 fields are shown (Figure 4B, lower). Since CQ inhibits lysosomal degradation by raising lysosomal pH, CQ treatment aids visualization of autophagosomes, which would be degraded during the incubation period. CQ treatment increased the number and area of LC3 puncta both under nutrient-rich and starving conditions. The increased and net values were greater in normal cells than in patient-derived cells; the areas of puncta ranged from 37.8 (None) to 52.4 (CQ) in control cells and from 9.6 (None) to 15.8 (CQ) in patient-derived cells under nutrient-rich conditions. This tendency was more prominent under starving conditions; the areas of puncta were 34.1 (EBSS) to 168.9 (EBSS CQ) in control cells and 21.0 (EBSS) to 112.6 (EBSS CQ) in patient-derived cells. This result clearly indicated that autophagosome formation was impaired in patient-derived RPE-like cells. However, it is uncertain whether *NEU1* deficiency directly leads to impaired autophagy or defective lysosomal activity resulting in perturbation of autophagy program.

Conclusion

Induced pluripotent stem (iPS) cells were generated from a type I sialidosis patient harboring a heterozygous missense mutation of c.239C>T and c.403G>A in the N-acetyl-α neuraminidase-1 (NEU1) gene, which product cleaves the terminal sialic acid residues in oligosaccharide chains of lipids and proteins. In sialidosis patients, decreased Neu1 activity leads to the accumulation of sialoglycoconjugates. Patients shows several manifestations including cherry red spot in the perifoveal region of retina, other than visual impairment, myoclonus, ataxia, seizure, mental retardation and hepatosplenomegaly. To investigate the pathological mechanism of cherry-red spot, retinal pigment epithelial (RPE) cells were induced from control and patient iPS cells. We observed that the patient RPE cells showed impaired autophagy flux with decreased formation of LC3 puncta. In addition, 3D culture of patient iPS cells resulted in the formation of vacuoles filled with lipid droplets and cellular components such as damaged mitochondria. These results indicated that Neu1 is pivotal for intracellular degradation system.

Acknowledgement

This study was supported in part by Research and Study Project of Tokai University General Research Organization and 2016-2017 Tokai University School of Medicine Project Research to T.Sato. A small part of the research was done using a grant from Kissei Pharmaceutical Co. Ltd. and Novartis. We would like to thank Editage (http://www.editage.jp) for English language editing. We thank to Dr. Yoshinori Okada and Ms. Yumi Iida for technical assistance.

Conflicts of Interest

A small part of the research was done using a grant from Kissei Pharmaceutical Co. Ltd. and Novartis.

References

1. Seyrantepe V, Poupetova H, Froissart R, Zabot MT, Maire I, et al. (2003) Molecular pathology of NEU1 gene in sialidosis. Hum Mutatio 22: 343-352.
2. Bonten EJ, Annunziata I, A d'Azzo (2014) Lysosomal multienzyme complex: Pros and cons of working together. Cell Mol Life Sci 71: 2017-2032.
3. Franceschetti S, Canafoglia L (2016) Sialidoses. Epileptic Disord 18: 89-93.
4. Sekijima Y, Nakamura K, Kishida D, Narita A, Adachi K, et al. (2013) Clinical and serial MRI findings of a sialidosis type I patient with a novel missense mutation in the NEU1 gene. Intern Med (Tokyo, Japan) 52: 119-124.
5. Michalewska Z, Gajos A, Michalewski J, Nawrocki J, Pshezhetsky AV, et al. (2011) Spectral optical coherence tomography in a patient with type I sialidosis. Med Sci Monit 17: CS129-CS131.
6. Frost LS, Mitchell CH, Boesze-Battaglia K (2014) Autophagy in the eye: Implications for ocular cell health. Exp Eye Res 124: 56-66.
7. Sinha D, Valapala M, Shang P, Hose S, Grebe R, et al. (2016) Lysosomes: Regulators of autophagy in the retinal pigmented epithelium, Exp Eye Res 144: 46-53.
8. Kim JY, Zhao H, Martinez J, Doggett TA, Kolesnikov AV, et al. (2013) Noncanonical autophagy promotes the visual cycle. Cell 154: 365-376.
9. Nakanishi M, Otsu M (2012) Development of Sendai virus vectors and their potential applications in gene therapy and regenerative medicine. Curr Gene Ther 12: 410-416.
10. Nishimura K, Sano M, Ohtaka M, Furuta B, Umemura Y, et al. (2011) Development of defective and persistent Sendai virus vector: A unique gene delivery/expression system ideal for cell reprogramming. J Biol Chem 286: 4760-4771.
11. Osakada F, Jin ZB, Hirami Y, Ikeda H, Danjyo T, et al. (2009) *In vitro* differentiation of retinal cells from human pluripotent stem cells by small-molecule induction. J Cell Sci 122: 3169-3179.
12. Hauselmann I, Borsig L (2014) Altered tumor-cell glycosylation promotes metastasis. Front Oncol 4: 28.
13. Uemura T, Shiozaki K, Yamaguchi K, Miyazaki S, Satomi S, et al. (2009) Contribution of sialidase NEU1 to suppression of metastasis of human colon cancer cells through desialylation of integrin beta4. Oncogene 28: 1218-1229.
14. Yogalingam G, Bonten EJ, van de Vlekkert D, Hu H, Moshiach S, et al. (2008) Neuraminidase 1 is a negative regulator of lysosomal exocytosis. Dev Cell 15: 74-86.
15. Meyer JS, Shearer RL, Capowski EE, Wright LS, Wallace KA, et al. (2009) Modeling early retinal development with human embryonic and induced pluripotent stem cells. Proc Natl Acad Sci U S A 106: 16698-16703.
16. Kuroda T, Yasuda S, Kusakawa S, Hirata N, Kanda Y, et al. (2012) Highly sensitive in vitro methods for detection of residual undifferentiated cells in retinal pigment epithelial cells derived from human iPS cells. PloS ONE 7: e37342.